Diruthenium Carbonyl Complexes Bound to Guaiazulene: Preparation and Thermally Reversible Photoisomerization Studies of Phosphine and Phosphite Derivatives of (μ_2,η^3:η^5-guaiazulene)$Ru_2(CO)_5$ and Iron Homologues

Kouki Matsubara,[†,§] Takashi Oda,[‡] and Hideo Nagashima*[,†,§,‡]

Institute of Advanced Material Study and Graduate School of Engineering Science, Kyushu University, Kasuga, Fukuoka 816-8580, Japan, and CREST, Japan Science and Technology Corporation (JST), Kyushu University, Kasuga, Fukuoka 816-8580, Japan

Received July 17, 2000

Preparation of a series of (μ_2,η^3:η^5-guaiazulene)$M_2(CO)_{5-n}(L)_n$ (M = Fe, Ru; n = 1, 2; L = phosphines and phosphites) was achieved by photochemical or thermal replacement of CO ligands in (μ_2,η^3:η^5-guaiazulene)$M_2(CO)_5$ [M = Fe (**1**) or Ru (**2**)], which exist as a mixture of two haptotropic isomers (**1-A** and **1-B**, **2-A** and **2-B**), by L, and the products were subjected to thermally reversible photoisomerization studies. Phosphine and phosphite derivatives of diiron complexes (μ_2,η^3:η^5-guaiazulene)$Fe_2(CO)_4(L)$ (**3**) and (μ_2,η^3:η^5-guaiazulene)$Fe_2(CO)_3(L)_2$ (**4**) were prepared in high yields by UV irradiation of **1** in the presence of L. In sharp contrast, (μ_2,η^3:η^5-guaiazulene)$Ru_2(CO)_4(L)$ (**5**) was successfully prepared by thermal replacement of a CO ligand in **2** by L. Although these derivatives may be formed as a mixture of two possible haptotropic isomers, only one isomer (**3-A**, **4-A**, and **5-A**) was isolated in each reaction. Detailed studies on the thermal substitution reaction of **2** revealed that formation of **5-A** from a mixture of **2-A** and **2-B** involved four elementary reactions: (1) the haptotropic rearrangement of **2-A** to **2-B**, (2) addition of L to **2-B** to form (μ_2,η^1:η^5-guaiazulene)$Ru_2(CO)_5(L)$ (**6**), (3) η^1 to η^3 haptotropic shift involving dissociation of CO to form a thermodynamically less stable haptotropic isomer of **5-B**, and (4) the haptotropic rearrangement of **5-B** to **5-A**. The intermediate **6** was isolated and completely characterized, whereas **5-B** was detected by spectroscopic methods. Isolation of **6** was accomplished by reaction of **2** with L at room temperature, which furnished selective conversion of **2-B** to **6** with **2-A** remaining intact. This reaction actually led to kinetic separation of **2-A** from a mixture of **2-A** and **2-B**, and complete characterization of **2-A** and **2-B** was made. Studies on the interconversion of haptotropic isomers of **2**, **3**, **4**, and **5** revealed the following: (1) the diiron complexes **3** and **4** were generally inactive toward the rearrangement; (2) in contrast to facile interconversion between **2-A** and **2-B**, the rearrangement of diruthenium compounds, **5**, was detectable only in a complex bearing a small phosphite ligand.

Introduction

Hapticity change of conjugated π-ligands increases flexibility of their coordination modes, leading to high reactivity toward ligand exchange processes and other organometallic reactions.[1−3] The haptotropic rearrangement, which is one of the interesting outcomes of the hapticity change, is slipping of a transition metal fragment from one coordination site to the other with total electron count remaining intact on a polyaromatic hydrocarbon or cyclic polyene ligand.[4,5] Although a number of studies on the haptotropic rearrangement in mononuclear transition metal compounds bearing such

[†] Institute of Advanced Material Study, Kyushu University.
[‡] Graduate School of Engineering Science, Kyushu University.
[§] CREST.

(1) For a review: O'Connor, J.; Casey, C. P. *Chem. Rev.* **1987**, *87*, 307.

(2) Collman, J. P.; Hegedus, L. S.; Norton, J. R.; Finke, R. G. *Principles and Applications of Organotransition Metal Chemistry*; University Science Books: Mill Valley, CA, 1987.

(3) Examples for the hapticity change affecting the reaction rates: (a) Rerek, M. E.; Basolo, F. *J. Am. Chem. Soc.* **1984**, *106*, 5908. (b) Forchner, T. C.; Cutler, A. R. *Organometallics* **1985**, *4*, 1247. (c) Forchner, T. C.; Cutler, A. R.; Kulling, R. K. *Organometallics* **1987**, *6*, 889, and references sited therein.

(4) For reviews: (a) Mann, B. E. In *Comprehensive Organometallic Chemistry*; Wilkinson, G., Stone, F. G. A., Abel, E. W., Eds.; Pergamon: Oxford; Vol. 3, Chapter 20, 1982. (b) Mann, B. E. *Chem. Soc. Rev.* **1986**, *15*, 167. (c) Albright, T. A.; Hofmann, P.; Hoffmann, R.; Lillya, C. P.; Dobosh, P. A. *J. Am. Chem. Soc.* **1983**, *105*, 3396. (d) Degenello, G. *Transition Metal Complexes of Cyclic Polyolefines*; Academic Press: London, 1982.

(5) Representative examples for the haptotropic rearrangement of mononuclear transition metal complexes: (a) Treichel, P. M.; Johnson, J. W. *Inorg. Chem.* **1977**, *16*, 749. (b) Kriss, R. U.; Treichel, P. M. *J. Am. Chem. Soc.* **1986**, *108*, 853. (c) Rerek, M. E.; Basolo, F. *Organometallics* **1984**, *3*, 647. (d) Nakasuji, K.; Yamaguchi, M.; Murata, I. *J. Am. Chem. Soc.* **1986**, *108*, 325. (e) Trifonova, O. I.; Ochertyanova, E. A.; Akhmedov, N. G.; Roznyatovsky, V. A.; Laikov, D. N.; Ustynyuk, N. A.; Ustynyuk, Y. K. *Inorg. Chim. Acta* **1998**, *280*, 328. (f) Oprunenko, Y. F.; Akhmedov, N. G.; Laikov, D. N.; Malyugina, S. G.; Mstislavsky, V. I.; Roznyatovsky, V. A.; Ustynyuk, Y. A.; Ustynyuk, N. A. *J. Organomet. Chem.* **1999**, *583*, 328. (g) Veiros, L. F. *J. Organomet. Chem.* **1999**, *587*, 221.

10.1021/om000608g CCC: $20.00
Publication on Web 02/03/2001

Scheme 1

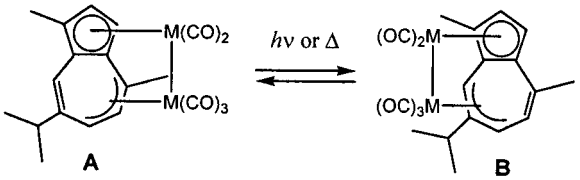

M = Fe (**1**) hν: 35 : 65
Δ: 55 : 45 (70~110°C)
M = Ru (**2**) hν: 46 : 54
Δ: 45 : 55 (35~60°C)

ligands have been undertaken both experimentally and theoretically,[4,5] only a few reports have been published on the rearrangement of the dinuclear systems.[6−8] Diiron and diruthenium carbonyl complexes ($\mu_2,\eta^3{:}\eta^5$-guaiazulene)$M_2(CO)_5$ [M = Fe (**1**) and Ru (**2**)] have two haptotropic isomers, **1-A** and **1-B** or **2-A** and **2-B**. Studies on CO scrambling processes were carried out by Cotton and co-workers in 1977, and the authors pointed out that thermal interconversion between those haptotropic isomers concomitantly took place.[7a] We recently reinvestigated this haptotropic rearrangement and reported that the rearrangement was induced both thermally and photochemically (Scheme 1).[7b]

The thermally reversible photoisomerization is an interesting entry to photofunctional molecules, and numerous studies on the organic photofunctional molecules have been carried out.[9] However, photoreactive organometallic compounds have not been fully explored[10−13] except for the elegant work on photoisomerization of ($\eta^5{:}\eta^5$-bicyclopentadienyl)$Ru_2(CO)_4$ to ($\mu_2,\eta^1{:}\eta^5$-cyclopentadienyl)$Ru_2(CO)_4$ reported by Vollhardt and co-workers,[10] in which the reverse isomerization was induced thermally with an enthalpy change of ca. −30 kcal/mol. The isomerization of **1** is a rare example of thermally reversible photoisomerization involving haptotropic rearrangement; however, it is problematic to us that there are small differences in the isomer ratios between that in the thermal equilibrium and that in the photostatic state. Vollhardt and co-workers reported interesting ligand effects in their thermally reversible photoisomerization of ($\eta^5{:}\eta^5$-bicyclopentadienyl)$Ru_2(CO)_4$ to ($\mu_2,\eta^1{:}\eta^5$-cyclopentadienyl)$Ru_2(CO)_4$.[10] Replacement of a CO ligand by PMe_3 completely inhibited the reaction, whereas introduction of less basic $P(OMe)_3$ successfully induced the photoisomerization. This prompted us to examine whether improvement of the isomer ratio may be possible by replacement of CO ligands in **1** or **2** by phosphines and phosphites.

Since Cotton and we reported that photochemical substitution of CO in **1** by PEt_3 resulted in formation of mono- and disubstituted complexes, ($\mu_2,\eta^3{:}\eta^5$-guaiazulene)$Fe_2(CO)_4(PEt_3)$ (**3b**) and ($\mu_2,\eta^3{:}\eta^5$-guaiazulene)-$Fe_2(CO)_3(PEt_3)_2$ (**4b**),[7] it was expected that application of this reaction to introduction of phosphines and phosphites would result in successful preparation of **3** and **4** bearing a wide variety of phosphines and phosphites (Scheme 2, eq 1). However, there has been no report on preparation of the corresponding ruthenium homologues, and development of their synthetic methods remains a problem to be solved.

In this paper, we wish to report that phosphine and phosphite derivatives of **2**, ($\mu_2,\eta^3{:}\eta^5$-guaiazulene)Ru_2-$(CO)_4$(L) (**5**), can successfully be synthesized by thermal substitution of a CO ligand in **2** by L [L = PMe_3, $P(OPh)_3$, and $P\{(OCH_2)_3CMe\}$], though photochemical procedures gave the product only in low yields (Scheme 2, eq 2).[7] These results are in sharp contrast to the fact that the ligand replacement of the diiron homologues successfully proceeded photochemically but not thermally. Thermal substitution reactions of **2** were studied in detail by isolation or detection of reaction intermediates. During these mechanistic studies, a novel separation method for two haptotropic isomers of **2** was discovered, which makes possible for the first time complete characterization of these isomers. Development of preparative methods for **2**, **3**, **4**, and **5** let us examine their photochemical and thermal isomerization behavior. In contrast to facile haptotropic rearrangement of **1** and **2**, most of the phosphine and phosphite derivatives were inactive toward the isomerization; however, we discovered as an important outcome of this study that a *ruthenium* derivative bearing a *small phosphite*, ($\mu_2,\eta^3{:}\eta^5$-guaiazulene)$Ru_2(CO)_4$(L) (**5g-A**), photochemically isomerized to a mixture of **5g-A** and **5g-B**, and we achieved complete thermal reverse isomerization to **5g-A** upon heating (Scheme 3).

Results and Discussion

Syntheses and Characterization of ($\mu_2,\eta^3{:}\eta^5$-guaiazulene)$Fe_2(CO)_4$(L) (3), ($\mu_2,\eta^3{:}\eta^5$-guaiazulene)-$Fe_2(CO)_3(L)_2$ (4), and ($\mu_2,\eta^3{:}\eta^5$-guaiazulene)Ru_2-$(CO)_4$(L) (5). As reported earlier, photoirradiation of **1**, either **1-A**, **1-B**, or their mixture in the presence of PEt_3, resulted in formation of mono- and disubstituted complexes, ($\mu_2,\eta^3{:}\eta^5$-guaiazulene)$Fe_2(CO)_4(PEt_3)$ (**3b**) and ($\mu_2,\eta^3{:}\eta^5$-guaiazulene)$Fe_2(CO)_3(PEt_3)_2$ (**4b**) (Scheme 2).[7] Using similar procedures, a series of compounds ($\mu_2,\eta^3{:}\eta^5$-guaiazulene)$Fe_2(CO)_4$(L) (**3**) and ($\mu_2,\eta^3{:}\eta^5$-guaiazulene)-$Fe_2(CO)_3(L)_2$ (**4**), where L = PMe_3, PEt_3, $PMePh_2$, PPh_3, $P(p\text{-Tol})_3$, PCy_3, $P\{(OCH_2)_3CMe\}$, and $P(OPh)_3$, was

(6) (a) Cotton, F. A.; Hunter, D. L.; Lahuerta, P. *Inorg. Chem.* **1975**, *14*, 511. (b) Churchill, M. R.; Wormald, J. *Inorg. Chem.* **1970**, *9*, 2239. (c) Nagashima, H.; Fukahori, T.; Itoh, K. *J. Chem. Soc., Chem. Commun.* **1991**, 786. (d) Nagashima, H.; Suzuki, A. *Kyushu Daigaku Kinou Busshitu Kagaku Kenkyusho Hokoku* **1997**, *11*, 175.

(7) (a) Cotton, F. A.; Hanson, B. E.; Kolb, J. R.; Lahuerta, P.; Stanley, G. G.; Stults, B. R.; White, A. J. *J. Am. Chem. Soc.* **1977**, *99*, 3673. (b) Nagashima, H.; Fukahori, T.; Nobata, M.; Suzuki, A.; Nakazawa, M.; Itoh, K. *Organometallics* **1994**, *13*, 3427.

(8) (a) Cotton, F. A.; Hunter, D. L.; Lahuerta, P. *J. Am. Chem. Soc.* **1975**, *97*, 1046. (b) Cotton, F. A.; Hunter, D. L. *J. Am. Chem. Soc.* **1975**, *97*, 5739.

(9) Photochromisms in organic chemistry: (a) Dürr, H.; Bouas-Laurent, H. *Photochromism*; Elsevier: Amsterdam, 1990. (b) Crano, J. C.; Guglielmetti, R. J. *Organic Photochromic and Thermochromic Compounds Vol. 1 and 2*; Kluwer Academic/Plenum: New York, 1999. (c) Wayne, R. P. *Principles and Applications of Photochemistry*; Oxford: New York, 1988.

(10) Bose, R.; Cammack, J. K.; Matzger, A. J.; Pflug, K.; Tolman, W. B.; Vollhardt, K. P. C.; Weidman, T. W. *J. Am. Chem. Soc.* **1997**, *119*, 6757.

(11) Thermally reversible photochemical isomerization of polynuclear clusters: (a) Adams, R. D.; Cortopassi, J. E.; Aust, J.; Myrick, M. *J. Am. Chem. Soc.* **1993**, *115*, 8877. (b) Yuki, M.; Okazaki, M.; Inomata, S.; Ogino, H. *Angew. Chem., Int. Ed. Engl.* **1998**, *37*, 2126.

(12) Isomerization of $Cp_2Fe_2(CO)_4$ and its derivatives, see: (a) Bruce, A. E.; Tyler, D. R. *Inorg. Chem.* **1984**, *23*, 3433. (b) Kawano, Y.; Tobita, H.; Ogino, H. *Organometallics* **1992**, *11*, 499, and references therein.

(13) Hughes briefly mentioned that photoinduced haptotropic rearrangement of Cp*Rh(1,2,5,6-$\eta^2{:}\eta^2$-C_8F_8) involves thermal reversal, and Vollhardt reported a photochemical and thermal haptotropic "walk" of CpCo(η^4-hexatriene-d_2). Detail studies, however, were not reported by either scientist. Hughes, R. P.; Carl, R. T.; Hemond, R. C.; Samkoff, D. E.; Reingold, A. L. *J. Chem. Soc., Chem. Commun.* **1986**, 306. King, J. A., Jr.; Vollhardt, K. P. C. *J. Organomet. Chem.* **1989**, *369*, 245.

Scheme 2

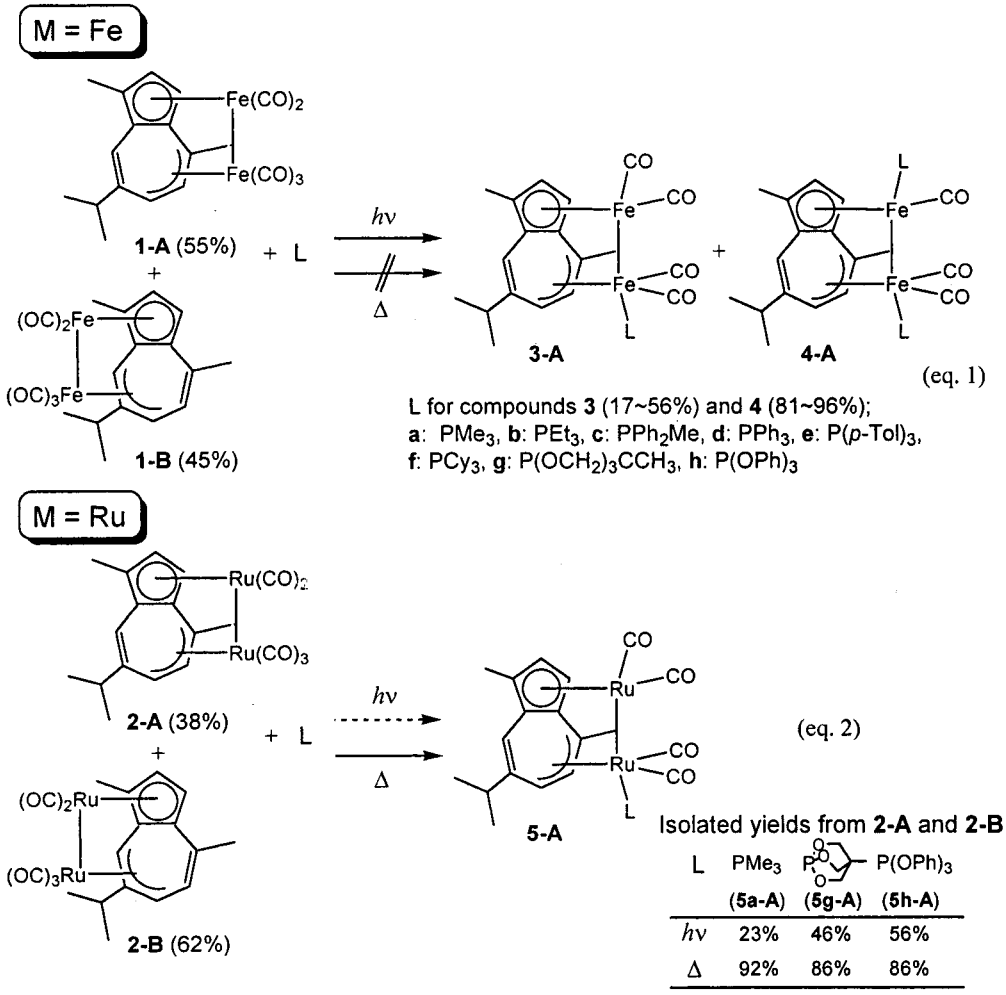

Scheme 3

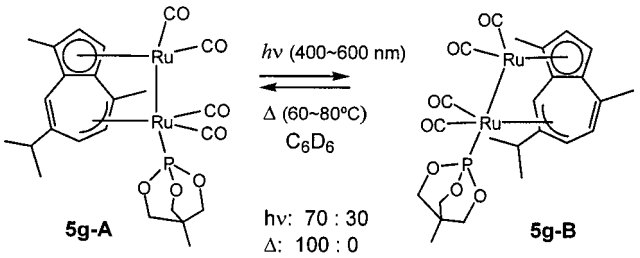

prepared.[14] The reaction rate was dependent on cone angles and basicity of L; bulky ligands decreased the rate especially in the second substitution from **3** to **4**, whereas reactions with less basic phosphites were faster than those with phosphines having similar cone angles.[14] In both **3** and **4**, only a single haptotropic isomer, **3-A** and **4-A**, respectively, was formed. Reaction profiles showed a typical stepwise formation of **3** and then **4**, of which the ratio (**3**: **4**) could be altered by changing the charged amount of L based on that of the starting carbonyl complex and the irradiation period. Attempted thermal replacement of CO ligands in **1** by L gave only a trace amount of **3**.

In sharp contrast to the fact that the photochemical ligand substitution of diiron compounds is superior to the thermal process, the thermal ligand replacement of the diruthenium compounds is a better method to produce the corresponding phosphine and phosphite derivatives than the photochemical reaction. Thus, photochemical substitution of CO ligands in **2** (a 38:62 mixture of **2-A** and **2-B**) by L is different from that of **1** in giving only the monosubstituted product **5**, where L = PMe_3 (**5a**), P{$(OCH_2)_3CMe$} (**5g**), and $P(OPh)_3$ (**5h**), only in low to moderate yields (23−56%) as shown in Scheme 2. The products exist as a single isomer (**5a-A**, **5g-A**, and **5h-A**, respectively). Preparation of **5** in excellent yields was achieved by a thermal replacement reaction; treatment of a 38:62 mixture of **2-A** and **2-B** with a phosphorus ligand (3 equiv to **2-A** + **2-B**), PMe_3, P{$(OCH_2)_3CMe$}, or $P(OPh)_3$, in C_6H_6 at 80 °C for 15 h results in formation of (μ_2,η^3:η^5-guaiazulene)$Ru_2(CO)_4$(L) (**5-A**) [L = PMe_3 (**5a-A**), P{$(OCH_2)_3CMe$} (**5g-A**), or $P(OPh)_3$ (**5h-A**)] in 86−92% yield (Scheme 2).

(14) There is substantial difference in the reaction rate between PEt_3 and $P(OPh)_3$, which have similar cone angles; the reactivity of less basic phosphites is higher than that of phosphines. These two factors sometimes affect the results of substitution: in the case of more basic and bulky PCy_3, the second substitution reaction was never observed, presumably because the high basicity lowered the rate of the substitution, and sterically bulky PCy_3 prevented formation of the disubstituted derivative. In contrast, small and less basic P{$(OCH_2)_3CMe$} quickly reacted with **1** to form **4g**: even formation of a trisubstituted complex, (μ_2,η^3:η^5-guaiazulene)$Fe_2(CO)_2$[P{$(OCH_2)_3CMe$}]$_3$, was suggested from the NMR evidence when **1** was irradiated for a long time in the presence of excess amounts of the phosphite. Details of this trisubstituted complex are described in the Supporting Information.

Table 1. Crystallographic Data for 5g-A, 6a, 2-A, and 2-B

	5g-A	6a	2-A	2-B
formula	$C_{24}H_{27}O_7PRu_2$	$C_{23}H_{27}O_3PRu_2$	$C_{20}H_{18}O_5Ru_2$	$2C_{20}H_{18}O_3Ru_2$
fw	660.57	616.56	540.48	540.48
temp, K	293(2)	223(2)	223(2)	293(2)
habit	yellow plate	orange prism	yellow prism	orange prism
cryst dimens, mm	0.30 × 0.14 × 0.12	0.40 × 0.30 × 0.10	0.50 × 0.40 × 0.20	0.24 × 0.21 × 0.15
cryst syst	monoclinic	orthorhombic	monoclinic	triclinic
space group	$P2_1/n$	$Pbca$	$P2_1/n$	$P\bar{1}$
a, Å	14.926(3)	25.5266(3)	13.627(2)	12.163(4)
b, Å	9.570(9)	15.335(2)	16.3608(2)	14.527(8)
c, Å	18.179(4)	12.393(2)	8.952(1)	11.391(8)
α, deg	90.26(5)			
β, deg	101.82(2)		96.39(1)	95.31(4)
γ, deg				97.36(4)
V, Å^3	2542(2)	4851.0(9)	1983.3(3)	1987(2)
Z	4	8	4	4
D_{calc}, g cm^{-3}	1.726	1.688	1.810	1.806
diffractometer	AFC-7R (Rigaku)	RAXIS II (Rigaku)	RAXIS II (Rigaku)	AFC-7R (Rigaku)
radiation (λ, Å)	Mo Kα (0.71070 Å)	Mo Kα (0.71070)	Mo Kα (0.71070)	Mo Kα (0.71070)
monochromator	graphite	graphite	graphite	graphite
μ_{calc}, cm^{-1}	12.92	13.41	15.50	15.47
F (000)	1320	2464	1064	1064
scan type	$\omega-2\theta$	$\omega-2\theta$	$\omega-2\theta$	$\omega-2\theta$
θ range, deg	$2.54 < \theta < 27.50$	$1.6 < \theta < 30.04$	$1.95 < \theta < 30.03$	$2.58 < \theta < 27.50$
no. of data collectd	6003	6058	5105	9120
no. of used data ($I > 2\sigma(I)$)	3026	5674	4886	3911
no. of variables	316	283	244	487
refinement method	full-matrix least-squares on F^2	full-matrix least-squares on F^2	full-matrix least-squares on F^2	full-matrix least-squares on F^2
GOF	0.966	1.265	1.132	1.003
R_1/wR_2 ($I > 2\sigma(I)$)	0.0528/0.1335	0.0451/0.1149	0.0403/0.1029	0.0768/0.1933
R_1/wR_2 (all)	0.1459/0.1669	0.0510/0.1175	0.0434/0.1048	0.2078/0.2701
$\Delta\rho$ max, e Å^{-3}	0.804 and −1.102	0.723 and −0.977	0.627 and −1.383	2.630 and −1.191

The compounds **3b** and **4b** have already been identified by spectroscopy in the literature.[7] Features in spectroscopy of the derivatives of **3** and **4** are similar to those observed for **3b** and **4b**, respectively.[7b] Typically, existence of $Fe(CO)_2L$ in **3** and Fe(CO)(L) and $Fe(CO)_2L$ in **4** can be identified by ^{31}P NMR. Characteristic P−C coupling was observed in ^{13}C resonances of the CO ligands. Coordination sites for the Fe(CO)(L) or $Fe(CO)_2L$ moiety were determined by typical P−H coupling (J_{PH} = 4−6 Hz) observed in ^1H resonances of the guaiazulene ligand. The NMR assignment was supported by X-ray structure of **3b**[7a] and that of **4e**.[15]

Spectral features of **5** are similar to **3**. For example, existence of $Ru(CO)_2L$ is evidenced by a single resonance appearing in ^{31}P NMR and two ^{13}C resonances due to the CO ligands which have typical P−C coupling (J_{PC} = 9.5 Hz for **5a-A**).[16] The P−H coupling (J_{PH} = 4−6 Hz for **5a-A**, **5g-A**, and **5h-A**) observed in two ^1H resonances of the guaiazulene ligand (H3 and H4) suggested η^3-allyl coordination of three carbons in the seven-membered ring. The molecular structure of **5g** unequivocally supported these assignments. Crystallographic data and representative bond distances and angles are summarized in Tables 1 and 2. The ORTEP drawing is illustrated in Figure 1. The metal−metal bond distance (Ru−Ru) is 2.873 (1) Å, which is similar to that in **2-A** and **2-B** but is longer than the Fe−Fe distances in **1-A**, **1-B**, and **3b-A** by 0.07−1.1 Å. The phosphite is coordinated to the Ru(2) atom with a bond distance of 2.224-(2) Å. The Ru(1), Ru(2), and P atoms make an angle of 169.91(6)°. Five carbons in the five-membered ring of the guaiazulene ligand, C1−C3, C9, and C10, are bonded with the Ru(1) atom, whereas C4−C6 are bound to the Ru(2) atom; the bond distances are 2.188(7)−2.308 (7) Å.

Table 2. Representative Bond Lengths (Å) and Angles (deg) of 5g-A

Ru(1)−Ru(2)	2.873(1)	Ru(2)−C(6)	2.281(8)
Ru(1)−C(1)	2.268(8)	Ru(2)−P(1)	2.224 (2)
Ru(1) −C(2)	2.248(9)	C(10)−C(4)	1.44(1)
Ru(1)−C(3)	2.251(9)	C(4)−C(5)	1.40(1)
Ru(1)−C(9)	2.253(7)	C(5)−C(6)	1.42(1)
Ru(1)−C(10)	2.259(8)	C(6)−C(7)	1.47(1)
Ru(2)−C(4)	2.308(7)	C(7)−C(8)	1.34(1)
Ru(2)−C(5)	2.188(7)	C(8)−C(9)	1.44(1)
Ru(1)−Ru(2)−P(1)	169.91(6)	P(1)−Ru(2)−C(18)	94.5(3)
Ru(1)−Ru(2)−C(18)	79.8(3)	P(1)−Ru(2)−C(19)	90.4(3)
Ru(1)−Ru(2)−C(19)	82.4(3)	Ru(1)−C(16)−O(1)	175(1)
Ru(2)−Ru(1)−C(16)	99.1(3)	Ru(1)−C(17)−O(2)	178(1)
Ru(2)−Ru(1)−C(17)	99.6(3)	Ru(2)−C(18)−O(3)	173(1)
C(16)−Ru(1)−C(17)	87.9(4)	Ru(2)−C(19)−O(4)	178(1)

Detailed Studies of the Thermal Substitution of 2. As noted above, thermal ligand replacement of the diruthenium precursor by phosphorus ligands proceeded smoothly, but that of the diiron compound did not. A clue to understanding this difference was available from the experiments to isolate and characterize the reaction intermediates. When the reaction of **2** with PMe_3 was monitored by ^1H NMR, concentration of **2-B** was quickly decreased, and thereafter that of **2-A** was slowly dimin-

(15) We carried out X-ray crystallography of a single crystal of **4e** containing an equimolar amount of tris(*p*-tolyl)phosphine oxide in the crystal. The final *R* index [$I>2\sigma(I)$] of the refinement was 0.1427, since the number of observed reflections [5057 ($I>2\sigma(I)$)] was somewhat less than enough for the final stage of the least-squares refinement. The resulting data of this solution are insufficient to discuss in detail; however, it is possible to show the connectivity of the atoms. The structure of **4e** suggests that two phosphorus ligands are bonded to each iron atom. The results are summarized in the Supporting Information.

(16) Because of the peak broadening due to the rapid scrambling of the CO ligands,[17] P−C coupling could not be determined for **5g-A** and **5h-A**.

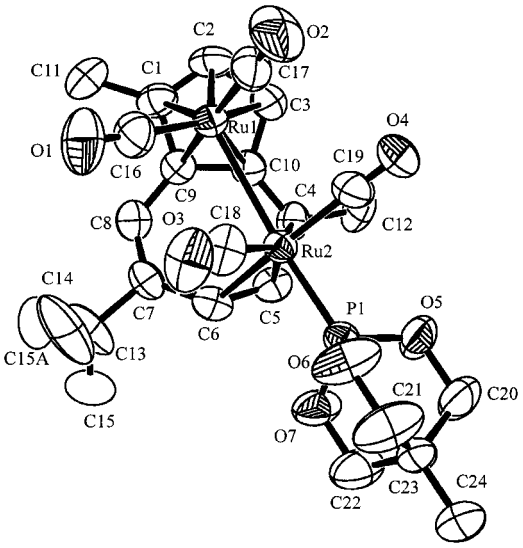

Figure 1. ORTEP drawing of **5g-A**. 50% probability of the thermal ellipsoids.

ished. Since the haptotropic rearrangement between **2-A** and **2-B** occurs at this temperature (Scheme 4, reaction I), the above result suggests that **5-A** was selectively formed from **2-B** and the reaction of **2-A** to **5-A** took place via the isomerization of **2-A** to **2-B**. Interestingly, formation of an intermediate was observed at an early stage of the reaction. Yield of the intermediate reached 29−33% after 3 h and decreased to 2−8% after 15 h.

This intermediate, ($\mu_2,\eta^1{:}\eta^5$-guaiazulene)$Ru_2(CO)_5$(L), **6a**, **6g**, or **6h**, was actually isolated when the reaction was carried out at room temperature, as shown in Scheme 4, reaction II. For example, treatment of a mixture of **2-A** and **2-B** (38:62) with PMe_3 (3 equiv to **2-B**) in benzene for 3 h results in complete conversion of **2-B** to **6a** with **2-A** remaining intact. Purification of the reaction mixture gave **6a** as crystals in 33% yield from a mixture of **2-A** and **2-B** (53% based on **2-B** reacted), whereas **2-A** was obtained in pure form in 28% yield. Using a similar procedure, the phosphite derivatives, **6g** and **6h**, were isolated in 38 and 37% (61 and 50% from **2-B**) yields, respectively.

Characterization of **6a**, **6g**, or **6h** was carried out by spectroscopy. Each compound has a single ^{31}P resonance (**6a**, δ −17.6 ppm; **6g**, δ 134.6 ppm; **6h**, δ 138.6 ppm) as a singlet. Their ^1H and ^{13}C NMR spectra showed that the proton assignable to H8 and the carbon due to C8 appeared at a characteristic upfield region (δ 3.1−3.2 ppm in ^1H NMR, around δ 15 ppm in ^{13}C NMR) (Table 3). The ^1H resonance appeared as a doublet with J_{PH} = 6−10 Hz. These data indicate the coordination of C8 to the ruthenium atom. Large P−C coupling (32−60 Hz) of the signal due to C8 suggested the phosphorus nucleus is bound to the ruthenium at the trans position of C8. No sign of coordination was seen in other ^1H or ^{13}C resonances due to protons and carbons in the seven-membered ring of the azulene ligand. Although ^{13}C resonances derived from the CO ligands were not visible

Scheme 4

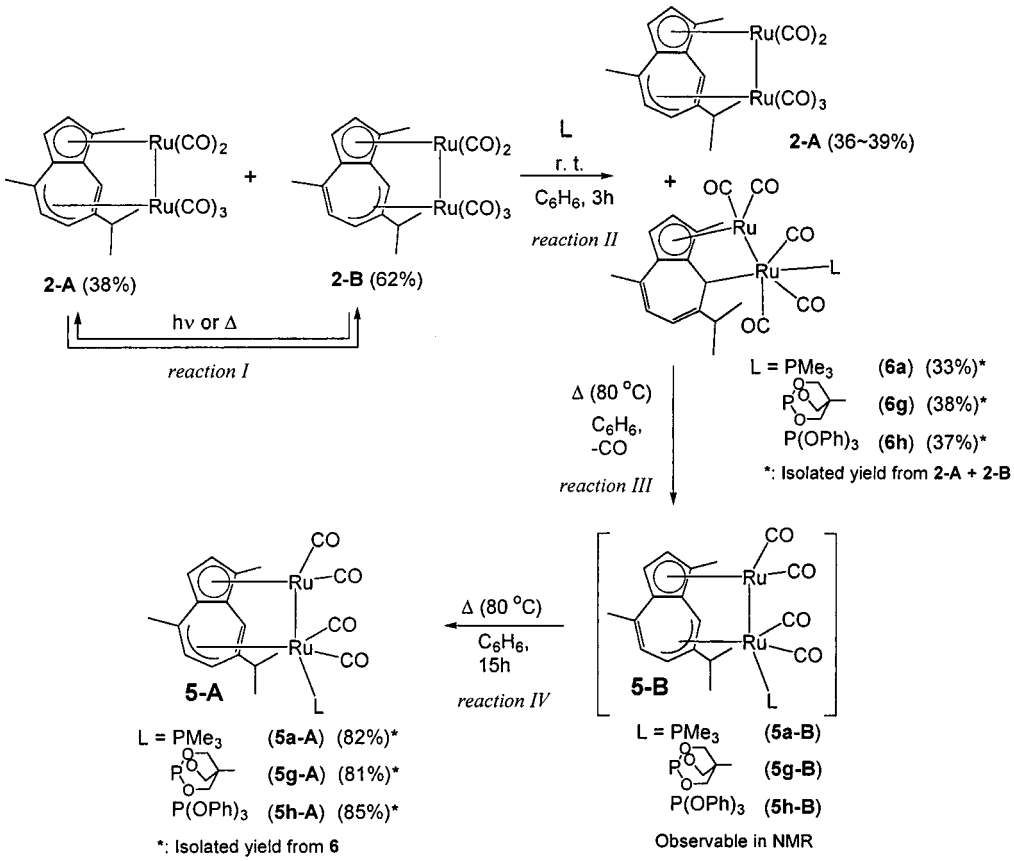

I) Haptotropic rearrangement, *II*) η^3 to η^1 conversion by addition of L, *III*) η^1 to η^3 conversion by elimination of CO, *IV*) Haptotropic rearrangement

Table 3. ^{1}H, ^{13}C, and ^{31}P NMR Spectral Data[a] of 6a, 6g, 6h[b]

	H2	H3	H5	H6	H8
6a	5.09, $^3J_{HH}$ = 2.9	4.92, $^3J_{HH}$ = 2.9	5.66, $^3J_{HH}$ = 7.8	5.26, $^3J_{HH}$ = 7.8, J_{PH} = 2.7	3.18, $^3J_{PH}$ = 6.2
6g	5.14, $^3J_{HH}$ = 2.9	4.97, $^3J_{HH}$ = 2.9	5.62, $^3J_{HH}$ = 7.8	5.24, $^3J_{HH}$ = 7.8, J_{PH} = 4.9	3.18, $^3J_{PH}$ = 10.4
6h	5.10, $^3J_{HH}$ = 2.9	4.94, $^3J_{HH}$ = 2.9	5.64, $^3J_{HH}$ = 7.3	5.25, $^3J_{HH}$ = 7.3, J_{PH} = 5.6	3.14, $^3J_{PH}$ = 10.4

	C2	C3	C5	C6	C8	PR_3
6a	86.0	80.0	130.0, $^5J_{PC}$ = 2.4	112.2, $^4J_{PC}$ = 5.0	15.3, $^2J_{PC}$ = 32	-17.6
6g	85.8	79.5	129.9, $^5J_{PC}$ = 4.0	112.3, $^4J_{PC}$ = 8.0	15.6, $^2J_{PC}$ = 55	134.6
6h	86.2	80,6	130.0, $^5J_{PC}$ = 5.0	113.1, $^4J_{PC}$ = 9.0	16.1, $^2J_{PC}$ = 60	138.6

[a] In C_6D_6. Chemical shifts (δ; ppm), coupling constant (J; Hz).

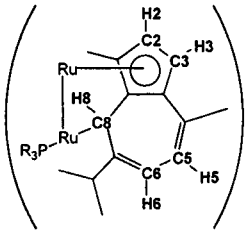

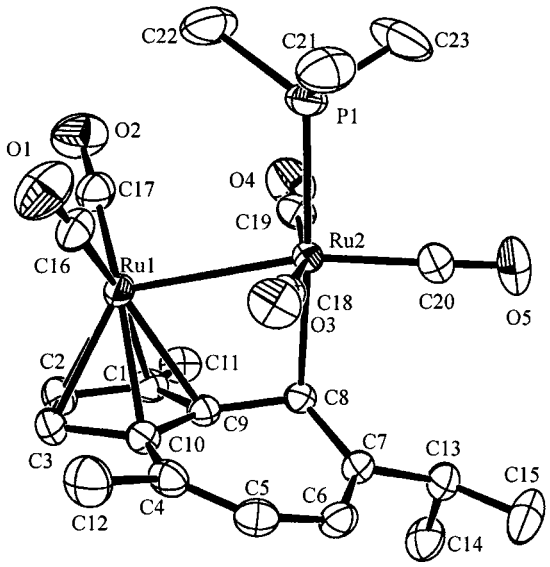

Figure 2. ORTEP drawing of **6a**. 50% probability of the thermal ellipsoids.

Table 4. Representative Bond Lengths (Å) and Angles (deg) of 6a

Ru1−Ru2	2.8380(4)	Ru2−P1	2.380(1)
Ru1−C1	2.256(4)	C10−C4	1.461(6)
Ru1−C2	2.249(4)	C4−C5	1.356(6)
Ru1−C3	2.241(4)	C5−C6	1.450(6)
Ru1−C9	2.264(4)	C6−C7	1.345(6)
Ru1−C10	2.255(4)	C7−C8	1.480(5)
Ru2−C8	2.280(4)	C8−C9	1.466(5)
Ru1−Ru2−C10	76.1(1)	P1−Ru2−C10	176.0(1)
Ru1−Ru2−P1	100.64(3)	Ru2−Ru1−C16	97.8(2)
Ru1−Ru2−C18	83.2(1)	Ru2−Ru1−C17	95.5(1)
Ru1−Ru2−C19	84.1(1)	C16−Ru1−C17	90.7(2)
Ru1−Ru2−C20	166.9(1)		

due to the rapid CO exchange processes,[17] five absorptions observed in the IR spectra suggest the existence of five of these ligands. These results are in accord with the structural features of **6a**, **6g**, or **6h**, described in Scheme 4. The molecular structure of **6a** unequivocally supports the structure suggested from spectroscopy as illustrated in Figure 2. Crystallographic data are summarized in Table 1, and representative bond lengths and angles are shown in Table 4. Carbons in the five-membered ring are bonded with Ru(1) by the π-cyclopentadienyl coordination mode. There is a carbon−ruthenium σ-bond between Ru(2) and C8, of which the distance is 2.280(4) Å. The guaiazulene ligand is bonded with diruthenium species with the $\mu_2,\eta^1{:}\eta^5$ coordination mode, which is similar to that seen in ($\mu_2,\eta^1{:}\eta^5$-4,5-dihydroacenaphthylene)$Ru_3H_2(CO)_7$.[18] PMe_3 was coordinated to Ru(2) by the Ru−P distance of 2.380(1) Å. Ligands of Ru(2), Ru(1), P, three CO's, and C8 make an octahedral arrangement, in which the P atom is located at the trans position of C8; this is in good agreement with the spectroscopic result described above.

Regeneration of the η^3-allyl moiety was achieved by thermal reaction of **6a**, **6g**, or **6h**, which induced liberation of a CO ligand, leading to quantitative formation of **5a-A**, **5g-A**, or **5h-A**, respectively (Scheme 4). The isolated yields of **5a-A**, **5g-A**, and **5h-A** were over 80% from **6a**, **6g**, or **6h**, respectively. These results provide experimental evidence supporting that formation of **5** from **2-B** proceeds by way of the η^1-allyl intermediate **6**.

The reaction from **6** to **5** requires further explanation. Besides the conversion of η^3 to η^1 coordination mode, the haptotropic shift leading to change of the coordination sites in the azulene ligand (C8 in **6**, C4−C6 in **5**) is apparently involved in this conversion from **6** to **5**. Detailed investigation on the thermal reaction of **6a**, **6g**, or **6h** gave NMR evidence suggesting existence of an intermediate, of which maximum yield reached 19, 53, and 9% in the reaction of **6a**, **6g**, and **6h**, respectively. ^{1}H, ^{13}C, and ^{31}P NMR spectra as well as C−H COSY and long-range C−H, P−H COSY spectra of the intermediate available in the reaction of **6g** are in accord with those of **5g-B**, which is one of the haptotropic isomers of **5g**. Similar spectroscopic features were also seen in **5a-B** and **5h-B**. These spectroscopic data suggest that the reaction from **6** to **5-A** involves dissociation of CO from **6** and concomitant η^1 to η^3 hapticity change of the allyl moiety to form **5-B (**Scheme 4, reaction III). Then, the thermal haptotropic rearrangement of **5-B** yields the final product **5-A (**Scheme 4, reaction IV).

Isolation of **5-B** has so far been unsuccessful because both **5-A** and **5-B** are extremely soluble in common organic solvents, which prevents separation of these two products by extraction or recrystallization. Attempted chromatographic separation by alumina, silica, and florisil decomposed these compounds. However, spectroscopic evidence i−iii is enough to assign this new compound as **5g-B**. The points of the summary illustrated in Figure 3 are as follows: (i) *The ^{31}P resonance.* The ^{31}P NMR spectrum of a 70:30 mixture of **5g-A** and **5g-B** in toluene-d_8 at −90 °C showed two peaks at 123.5 and 122.8 ppm in a ratio of 3:1. The former corresponds to a signal derived from **5g-A**, and the latter is assignable to **5g-B** (A in Figure 3). (ii) *The*

(17) Rapid scrambling of CO ligands in the diiron complexes having bridging polyene and polyenyl ligands were studied in detail: (a) Ref 6a. (b) Cotton, F. A.; Hanson, B. E.; Kolb, J. R.; Lahuerta, P. *Inorg. Chem.* **1977**, *16*, 89.

(18) Nagashima, H.; Fukahori, T.; Aoki, K.; Itoh, K. *J. Am. Chem. Soc.* **1993**, *115*, 10430.

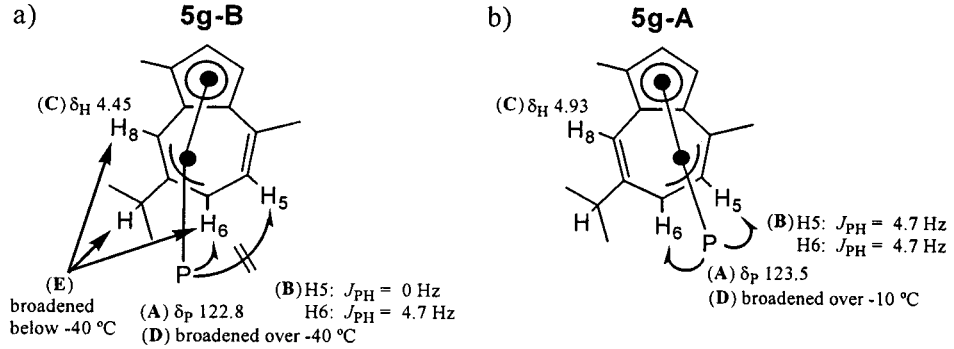

Figure 3. Comparison of spectroscopic data between (a) **5g-B** and (b) **5g-A**. (A) The ^{31}P resonance. (B) Long-range PH coupling. (C) High-field shift of the H8 proton. (D) Temperature-dependent phenomena in ^{31}P NMR. (E) Temperature-dependent phenomena in ^{1}H NMR.

long-range PH coupling. Peak splitting derived from long-range coupling between ^{1}H and ^{31}P ($J_{PH} = 4.7$ Hz) was observed at ^{1}H resonances of H5 and H6 in **5g-A** at room temperature, whereas no $^{1}H-^{31}P$ coupling was observed in the H8 resonance.[19] In contrast, clear $^{1}H-^{31}P$ long-range coupling was only visible at the H6 of **5g-B** ($J_{PH} = 4.7$ Hz), whereas no $^{1}H-^{31}P$ coupling was observed in the H5 resonance (B in Figure 3).[19] Although the $^{1}H-^{31}P$ long-range coupling was not clearly visible, the H8 resonance of **5g-B** showed higher field shift (Δ −0.5 ppm) than that of **5g-A** (C in Figure 3). (iii) *Temperature-dependent phenomena in ^{1}H and ^{31}P NMR.* The ^{31}P resonance of **5g-A** broadened at over 0 °C, whereas extensive broadening of the signal of **5g-B** was observed at over −60 °C. The broadening of the ^{31}P signals indicates a rapid exchange process of the coordinated CO and phosphite ligands (D in Figure 3). In the ^{1}H NMR spectrum of **5g-B**, the broadening of the peaks corresponding to the H6 and H8 resonances was observed at low temperatures (< −40 °C). This is in sharp contrast to the result that neither change of the chemical shift nor the broadening of the signal was seen in the H5 resonance of **5g-B**. Interestingly, broadening of the signals was also seen at the methyne proton of the ^{i}Pr group in **5g-B**, which was never seen at the methyne proton of the ^{i}Pr group in **5g-A** (E in Figure 3). These temperature-dependent phenomena of the signals from H6, H8, and the CH protons of the ^{i}Pr group could be related to the phosphite−CO ligand exchange process of **5g-B** described above. Such phenomena seen at H6, H8, and the CH protons of the ^{i}Pr group but not H5 strongly indicate that the $Ru(CO)_2(L)$ moiety is located at a position spatially close to H6, H8, and the CH of ^{i}Pr.

Chemical shift of the ^{13}C resonances of **5g-B** shown in Table 5 is more clear evidence supporting the structure of **5g-B**. The ^{13}C resonances of C4−C8 in **5g-B** were unequivocally assigned with the aid of H−C COSY (HMQC) and the long-range H−C COSY (HMBC) spectra. The ^{13}C NMR data of **5g-A** and those of two isomers of (μ_2,η^3:η^5-guaiazulene)$Ru_2(CO)_5$, **2-A** and **2-B**, are also shown for comparison. In these complexes, ^{13}C resonances bound to the ruthenium moiety showed a clear upfield shift by 28−46 ppm compared with those of uncoordinated carbons. Apparently there are similarities in chemical shifts of these carbon signals between **2-B** and **5g-B** and also between **2-A** and **5g-A**. In other words, δ-values of the ^{13}C resonances indicate that either C6−C8 in **2-B** and **5g-B** or C4−C6 in **2-A** and **5g-A** are bonded with the ruthenium moiety. Since **2-A** and **2-B** were successfully isolated and characterized by spectroscopy and crystallography as described above, this similarity in the carbon resonance is good evidence to support the structure of **5g-B**.

Table 5. ^{13}C NMR Resonances (δ; ppm) of the Guaiazulene Ligand of 2-A, 2-B, 5g-A, and 5g-B[a] in CD_2Cl_2 at 293 K

	C4	C5	C6	C7	C8
2-A	74.9	81.3	45.8	148.2	108.0
5g-A	70.6	81.0	45.4	148.6	106.5
2-B	110.2	125.7	51.1	123.3	51.5
5g-B	106.9	127.3	49.0	120.9	49.5

[a] C4−C8: see the number of the carbons in Figure 1 or Figure 6.

The above results provide unequivocal experimental evidence for four elementary reactions shown in reactions I−IV of Scheme 4, which may be involved in the conversion of **2** to **5.** Actual involvement of these four elementary reactions is supported by the result that the reaction of isolated **2-A** with the phosphorus ligand followed a typical pattern of sequential reactions; ^{1}H NMR spectra of the reaction mixture showed formation and disappearance of all of **2-B**, **6**, and **5-B** and formation of the final product **5-A**. The difference in thermal substitution between the diiron complex and the diruthenium homologue may be attributed to facile η^3 to η^1 conversion of **2** by coordination of L. In fact, attempted reaction of **1** with L did not give the corresponding η^1-complex at all. Conversion of η^3 to η^1-allyl species is often seen in group VIII transition metal complexes;[20] in organoruthenium chemistry, several examples of the η^3 to η^1 conversion of allyl ligands were reported for only mononuclear ruthenium complexes.[21] This is the first example to show the η^3 to η^1 hapticity change during

(19) The $^{31}P-^{1}H$ coupling was supported by $^{31}P-^{1}H$ long-range COSY spectra (HMBC) of **5g-A** and **5g-B**.

(20) (a) Faller, J. W. *Adv. Organomet. Chem.* **1977**, *16*, 211. (b) Fish, R. W.; Giering, W. P.; Marten, D.; Rosenblum, M. *J. Organomet. Chem.* **1976**, *105*, 101. (c) Gibson, D. H.; Hsu, W.-L.; Steinmetz, A. L. *J. Organomet. Chem.* **1981**, *208*, 89. (d) Faller, J. W.; Johnson, B. V.; Dryja, T. P. *J. Organomet. Chem.* **1974**, *65*, 395.

(21) (a) Sbrana, G.; Braca, G.; Benedetti, E. *J. Chem. Soc., Dalton Trans.* **1975**, 754. (b) Barnard, C. F. J.; Daniels, J. A.; Holland, P. R.; Mawby, R. J. *J. Chem. Soc., Dalton Trans.* **1980**, 2418. (c) Lehmkuhl, H.; Mauermann, H.; Benn, R. *Liebigs Ann. Chem.* **1980**, 754. (d) Nagashima, H.; Mukai, K.; Shiota, Y.; Yamaguchi, K.; Ara, K.; Fukahori, T.; Suzuki, H.; Akita, M.; Moro-oka, Y.; Itoh, K. *Organometallics* **1990**, *9*, 799.

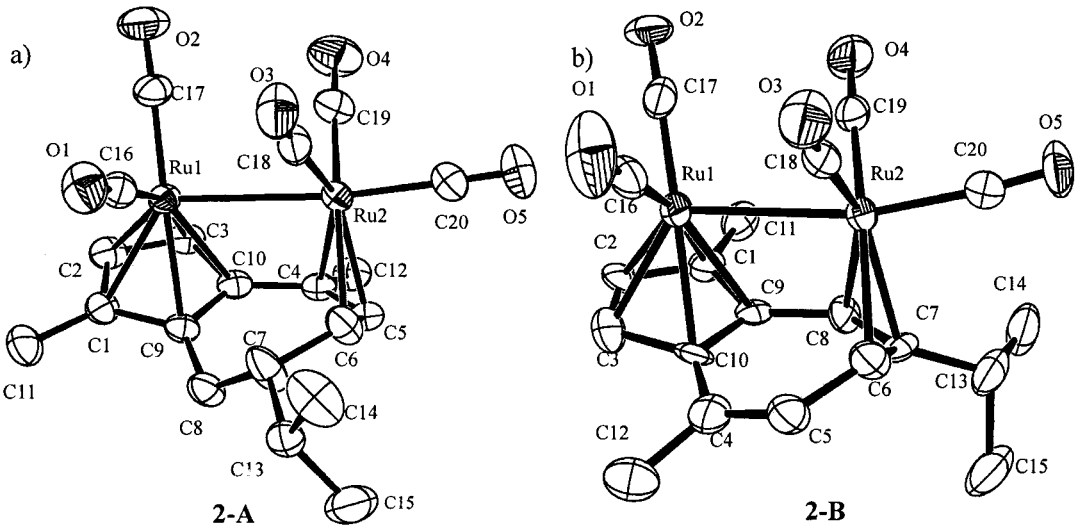

Figure 4. ORTEP drawing of **2-A** and **2-B**. 50% probability of the thermal ellipsoids: (a) **2-A**, (b) **2-B**.

Table 6. Representative Bond Lengths (Å) and Angles (deg) of 2-A and 2-B

	(a) bond lengths			(b) bond angles	
	2-A	**2-B**		**2-A**	**2-B**
Ru1−Ru2	2.8795(5)	2.894(2)	Ru1−Ru2−C8	94.1(1)	97.4(4)
Ru1−C1	2.268(3)	2.21(1)	Ru1−Ru2−C9	100.8(1)	104.9(4)
Ru1−C2	2.242(3)	2.22(1)	Ru1−Ru2−C10	77.67(9)	78.2(3)
Ru1−C3	2.233(3)	2.25(1)	Ru1−C16−O1	177.4(4)	175(1)
Ru1−C4	2.259(3)	2.24(1)	Ru1−C17−O2	176.0(3)	179(2)
Ru1−C5	2.251(3)	2.22(1)	Ru1−C18−O3	171.8(3)	178(1)
Ru2−C8	2.256(4)	2.25(2)	Ru1−C19−O4	177.3(3)	172(2)
Ru2−C9	2.197(3)	2.23(1)	Ru1−C20−O5	177.9(4)	173(1)
Ru2−C10	2.336(3)	2.29(1)			
C5−C6	1.477(5)	1.45(2)			
C6−C7	1.421(5)	1.36(2)			
C7−C8	1.510(5)	1.46(2)			
C8−C9	1.444(5)	1.39(2)			
C9−C10	1.409(5)	1.43(2)			
C4−C10	1.462(5)	1.48(2)			

ligand substitution in the dinuclear complex of ruthenium to our knowledge.

Kinetic Separation of 2-A from a Mixture of 2-A and 2-B. As described above, the haptotropic rearrangement between two isomers of ($\mu_2,\eta^3{:}\eta^5$-guaiazulene)-$M_2(CO)_5$, (**1**, M = Fe; **2**, M = Ru**)** was induced both thermally and photochemically.[7] Although two isomers of the diiron complex were successfully isolated[7a] and subjected to studies of the haptotropic rearrangement, complete separation of isomers of the diruthenium homologue, **2-A** and **2-B**, was difficult.[7b] Thus, detailed studies of the rearrangement have not yet been undertaken. As described above, the reaction of a mixture of **2-A** and **2-B** with phosphorus ligands at room temperature results in complete conversion of **2-B** to **6** with **2-A** remaining intact (Scheme 4, *reaction II*). This reaction eventually makes possible kinetic separation of **2-A** from a mixture of **2-A** and **2-B**. In a typical example, a 38:62 mixture of **2-A** and **2-B** was treated with PMe_3 (3 equiv to **2-B**) at room temperature for 3 h to give a mixture of **2-A** (38%) and **6** (59%). After removal of free PMe_3 and the solvent, the solid material was extracted with pentane. From the extracts, **2-A** was isolated in 28% yield as yellow crystals.

A crystal of **2-A** suitable for X-ray structure determination was available from a mixture of CH_2Cl_2 and pentane. Although isolation of a bulk quantity of **2-B** has not yet been successful, a pale orange crystal of **2-B** for structure determination was separated from a mixture of crystals of **2-A** and **2-B**. The ORTEP drawings are illustrated in Figure 4. Tables 1 and 6 present summarized crystallographic data as well as representative bond distances and angles of **2-A** and **2-B**. The Ru−Ru bond distance of **2-A** is 2.8795(5) Å, and that of **2-B** is 2.894(2) Å. The $Ru_2(CO)_5$ moiety was bound to the guaiazulene ligand with the $\mu_2,\eta^3{:}\eta^5$-coordination mode with Ru−C distances of 2.20−2.29 Å. In the diiron homologues, **1-A** and **1-B**, the Fe−Fe bond distances are 2.80(1) and 2.78(1) Å, respectively, and Fe−C(guaiazulene) distances are 2.05−2.20 Å. Variation in metal−metal and metal−carbon bond distances provides substantial difference in deviation of the guaiazulene ligand between the diruthenium compounds and diiron homologues. The NMR and IR data for **2-A** and **2-B** were in accord with the molecular structures.

Thermally Reversible Photoisomerization Studies of 2, 3, 4, and 5. The above-described results made possible successful isolation of a bulk quantity of **2-A**, **3-A**, **4-A**, and **5-A**. This led to studies on thermal and photochemical haptotropic rearrangement of these compounds (Scheme 5). In the interconversion between **2-A** and **2-B**, the equilibrium constant ([K_{eq} = [**2-B**]/[**2-A**]] determined by ^{1}H NMR was 1.23 ± 0.2 at 308, 313, 318, and 323 K. The kinetic data could be treated in terms of reversible first-order kinetics, and observed rate constants were 0.85 ± 0.05, 1.7 ± 0.1, 3.7 ± 0.2, and

Scheme 5

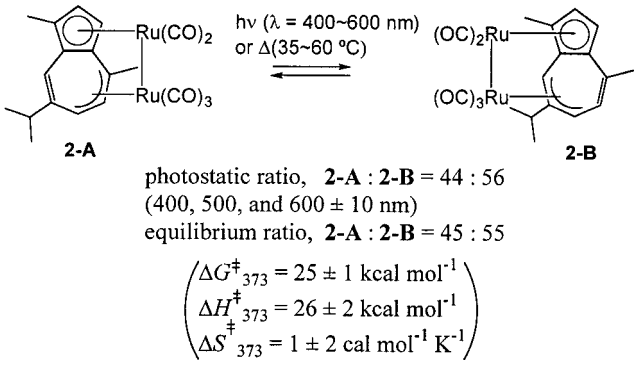

photostatic ratio, **2-A** : **2-B** = 44 : 56
(400, 500, and 600 ± 10 nm)
equilibrium ratio, **2-A** : **2-B** = 45 : 55

$$\begin{pmatrix} \Delta G^{\ddagger}_{373} = 25 \pm 1 \text{ kcal mol}^{-1} \\ \Delta H^{\ddagger}_{373} = 26 \pm 2 \text{ kcal mol}^{-1} \\ \Delta S^{\ddagger}_{373} = 1 \pm 2 \text{ cal mol}^{-1}\text{ K}^{-1} \end{pmatrix}$$

6.5 ± 0.3 (× 10^6) s^{-1} at 308, 313, 318, and 323 K, respectively. The calculated values of activation parameters are $\Delta G^{\ddagger}_{373} = 25 \pm 1$ kcal mol^{-1}, $\Delta H^{\ddagger}_{373} = 26 \pm 2$ kcal mol^{-1}, $\Delta S^{\ddagger}_{373} = 1 \pm 2$ cal mol^{-1} K^{-1}. Photochemical interconversion using UV interference filters (400, 500, 600 ± 10 nm) revealed that the rate of the reaction decreased in the order 400 > 500 > 600 nm, whereas there was no substantial difference in the isomer ratios at the photostatic states (1.26 ± 0.4).[22]

Attempted isomerization of a C_6D_6 solution of the diiron compounds, **3a**, **3b**, **3f**, **3g**, **3h**, **4a**−**4e**, or **4g**−**4h** under irradiation by a 450 W high-pressure Hg lamp for 10−18 h was unsuccessful. Thermal isomerization was also examined by heating the C_6D_6 solution at 60−110 °C for 5−15 h, but again we saw no sign of isomerization. Similarly, photoirradiation (450 W high-pressure Hg lamp) or heating (60−110 °C) of a solution of the diruthenium derivatives, **5a** and **5h**, did not induce the haptotropic isomerization. A breakthrough was achieved in the photoirradiation of **5g**. Photolysis of a C_6D_6 solution of **5g** (only a single isomer **5g-A**) by a 450 W high-pressure Hg lamp at room temperature for 10 h caused substantial color change of the solution from yellow to orange. The ^{1}H NMR spectrum of this solution revealed that it contained two products: the starting isomer **5g-A** and a new compound in a ratio of 70:30. Spectroscopic data of this new compound coincides with the haptotropic isomer **5g-B** (Scheme 1, eq 2).

Dependence of the ratio of photochemical isomerization of **5g-A** to the mixture of **5g-A** and **5g-B** on the wavelength was examined in detail using UV-interference filters. The isomer ratios of **5g-B** to **5g-A** at the photostatic states were 0.29, 0.20, and 0.28 ± 0.02 at 400, 500, and 600 ± 10 nm, respectively. Thermal reversion from the mixture of **5g-A** and **5g-B** proceeded at over 40, 60, 80, and 110 °C to result in complete regeneration of **5g-A** after 18, 12, 8, and 3 h, respectively. This photoisomerization/thermal reversion cycle, which was accompanied by the reversible color change between yellow and orange, could be repeated several times, though partial decomposition of the compounds (~3%) concomitantly occurred at each photochemical isomerization step.

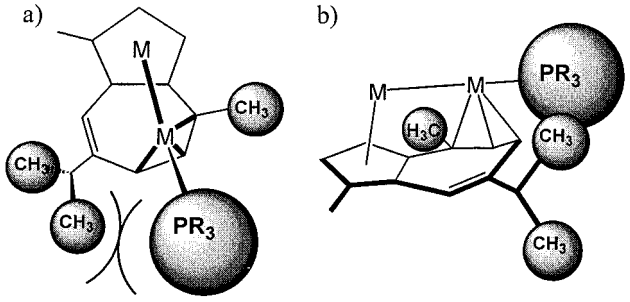

Figure 5. Steric repulsion between the phosphorus ligand and the isopropyl group in the guaiazulene ligand preventing isomerization: (a) top view, (b) side view.

Mechanistic Considerations. The above-described results suggest that thermally reversible photoisomerization of phosphine or phosphite derivatives of (guaiazulene)$M_2(CO)_5$ is possible in principle. However, the data so far obtained show that only a diruthenium complex bearing one small phosphite successfully undergoes the isomerization.[23] Thus, ruthenium as the metal and P{$(OCH_2)_3$CMe} as the sterically not bulky and electronically less basic phosphorus ligand are important factors for the isomerization. In the molecular structures of **3b-A** and **4e-A**, the phosphorus ligand is located between methyl and isopropyl substituents of the azulene ligand.[7a,15] Steric repulsion between the $Fe(CO)_2(L)$ moiety and the bulky isopropyl group probably prevents the isomerization from **3b-A** to **3b-B** and **4e-A** to **4e-B**. This steric problem is apparently one reason many of the derivatives described in this paper did not provide the haptotropic isomer.

In the diiron complexes, the isomerization did not occur even in those bearing small phosphorus ligands such as PMe_3 and P{$(OCH_2)_3$CMe}. In contrast, the diruthenium derivative bearing PMe_3 did not undergo the isomerization, but that having P{$(OCH_2)_3$CMe} actually gave the corresponding haptotropic isomer. We believe there are two reasons for this difference. One is a difference in the metal−metal bond distance between the diiron and diruthenium complexes; the Ru−Ru bond is longer than the Fe−Fe bond. The shorter Fe−Fe bond results in greater deviation of the azulene ligand from the planar structure, leading to an increase of the steric repulsion between the metal moiety and the methyl and isopropyl substituents, as shown in Figure 5.

The other factor is basicity of the phosphorus ligand. Successful isomerization of **5g** and unsuccessful conversion of **5a** can be attributed to the fact that introduction of basic phosphines somehow inhibits the isomerization. Vollhardt and co-workers suggested in their photoisomerization of (fulvalene)$Ru_2(CO)_3L$ that introduction of basic phosphine makes the Ru−Ru bond stronger, leading to inhibition of the photoisomerization.[10] Although further investigation is required to identify the

(22) The interconversion studies of **2-A** provide the following interesting points in comparison with the haptotropic rearrangement of the diiron homologues **1-A** and **1-B**. First, thermodynamic stability of the two isomers is **2-B** > **2-A**, whereas **1-A** > **1-B**. Second, the $\Delta S^{\ddagger}$ value for the interconversion between **2-A** and **2-B** is much larger than that observed in the haptotropic interconversion between **1-A** and **1-B**. There is a substantial difference in the metal−metal bond length between the diiron and diruthenium compounds, which leads to differences in deviation of the guaiazulene ligand from the planar structure and steric repulsion of methyl or isopropyl substituents of the guaiazulene ligand with metallic species. Although various mechanistic considerations have been undertaken on the basis of molecular structure, no clear explanation is yet available.

(23) Cone angle (deg) and χ (cm^{-1}) as steric and electronic factors of PR_3 reported by C. A. Tolman (Tolman, C. A. *Chem. Rev.* **1977**, *77*, 319): PMe_3, 118° and 2.6 cm^{-1}; P{$(OCH_2)_3$CMe}, 101° and 10.3 cm^{-1}; $P(OPh)_3$, 128° and 9.7 cm^{-1}.

isomerization mechanism of our system, Vollhardt's suggestion of Ru−Ru strength affecting the photoisomerization may also apply to our system. In other words, photoisomerization may involve photochemical fission of the Ru−Ru bond as an elementary reaction.

Conclusion

We described in this paper the successful synthesis of a series of phosphine and phosphite derivatives by photochemical and thermal ligand substitution in (μ_2,η^3:η^5-guaiazulene)$Ru_2(CO)_5$ and an iron homologue, and examination of thermally reversible photoisomerization of these derivatives. The reaction of **2** with phosphorus ligands provides three novel aspects for reaction chemistry of diruthenium compounds bound to guaiazulene. First, thermal substitution in the ruthenium complex **2** efficiently gives **5-A** in high yields, though that in the iron complex **1** affords only **3-A** in low yields. Second, formation of **5-A** from **2** proceeds through a remarkably multistep pathway involving reactions I−IV as shown in Scheme 4. All four of these processes involve facile hapticity change of the guaiazulene ligand; in other words, the facile hapticity change plays a critical role in ligand substitution reactions of polynuclear complexes bearing conjugated π-ligands. Third, **2-A** was kinetically separated from a mixture of **2-A** and **2-B**, providing a method for preparation of a bulk quantity of **2-A** in pure form; this, in turn, allowed detailed studies on its structure, photochemical interconversion (wavelength dependence on the ratio of the photochemical isomerization), and determination of thermodynamic parameters for thermal haptotropic isomerization from **2-A** to a mixture of **2-A** and **2-B**. Comparison of these data with the diiron homologue, **1-A** and **1-B**, gave interesting aspects of differences in structure and reactivity between the diiron and diruthenium compounds.

Derivatives **3**, **4**, and **5** were subjected to studies on thermally reversible photoisomerization, leading to the discovery that the diruthenium derivative **5g** bearing a small and less basic phosphorus ligand can successfully isomerize. The results indicate that derivatives of (μ_2,η^3:η^5-azulene)$Ru_2(CO)_4(L)$, where azulene is unsymmetrically substituted, can be generally useful for the thermally reversible photoisomerization, if the complex has *a substituted azulene ligand* bearing a substituent of appropriate size at relevant positions and *sufficiently small and less basic phosphorus ligands*. We see this as an interesting guideline, from which we can develop photofunctional organometallic molecules based on the haptotropic rearrangement, and further investigation to synthesize (μ_2,η^3:η^5-substituted azulene)$Ru_2(CO)_4(L)$ is currently underway.

Experimental Section

General Method. All experiments were carried out under an argon atmosphere using standard Schlenk techniques. Ether, THF, benzene, toluene, heptane, hexane, and benzene-d_6 were distilled from benzophenone ketyl and stored under argon atmosphere. P{$(OCH_2)_3$CMe} was prepared from $P(OMe)_3$ and 1,1,1-tris(hydroxymethyl)ethane.[24] Other reagents, solvents, and phosphorus ligands were used as received. NMR spectra were taken with a JEOL Lambda 400 or 600 spectrometer. Chemical shifts were recorded in ppm from the internal standard (^{1}H, ^{13}C: solvent) and the external standard (^{31}P: H_3PO_4). IR spectra were recorded in cm^{-1} on a JASCO FT/IR-550 spectrometer. The iron and ruthenium complexes **1**, **2**, **3b**, and **4b** were prepared according to the published methods.[7] Photochemical preparation of **3** and **4** was performed with procedures similar to those used for the preparation of **3b** and **4b**. Experimental details of these new diiron derivatives are described in the Supporting Information. The number of protons (H1−H8) and carbons (C1−C8) on the guaiazulene ligand is shown in Figure 6. Photochemical substitution in **1** and **2** was carried out with a Riko 400 W high-pressure Hg lamp, whereas the photochemical rearrangements in **2** and **5g** were examined with an Ushio 450W high-pressure Hg lamp and an Ushio 500 W xenon lamp.

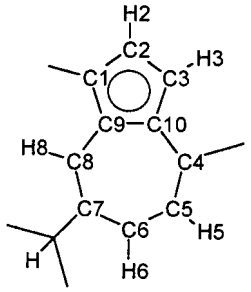

Figure 6. Number of protons (H1−H8) and carbons (C1−C8) of the guaiazulene ligand on the iron and ruthenium complexes **2-A**,**B**, **3-A**, **4-A**, **5-A**,**B**, and **6**.

General Procedure for Preparation of 5-A from a Mixture of 2-A and 2-B. In a typical example, a mixture of **2-A** and **2-B** (50.7 mg, 0.092 mmol) was dissolved in C_6H_6 (20 mL), and P{$(OCH_2)_3CCH_3$} (13.2 mg, 0.089 mmol) was added at room temperature. The mixture was heated at 80 °C for 15 h. After removal of the solvent in vacuo, the residual products were washed with pentane several times: the yield of **5g-A** was 56.0 mg (86%). Using similar procedures, **5a-A** (92%) and **5h-A** (86%) were isolated. Alternatively, photochemical preparation of **5-A** can be achieved in low to moderate yields. In a typical example, a mixture of **2-A** and **2-B** (50.3 mg, 0.092 mmol) and P{$(OCH_2)_3CCH_3$} (12.9 mg, 0.087 mmol) in benzene (20.0 mL) was irradiated for 15 h. After removal of the solvent in vacuo, the residue was washed by pentane to yield **5g-A** (28 mg, 46%). Using similar procedures, **5a**−**A** (23%) and **5h-A** (56%) were also obtained.

5a-A: yellow crystals, mp 141−4 °C (dec). ^{1}H NMR: δ 5.31 (d, J_{HH} = 2.9 Hz, 1H, H2), 5.07 (d, J_{HH} = 1.6 Hz, 1H, H8), 4.09 (dd, J_{HH} = 8.0 Hz, J_{PH} = 8.0 Hz, 1H, H5), 3.29 (d, J_{HH} = 2.9 Hz, 1H, H3), 2.37 (ddd, J_{HH} = 1.6, 8.0 Hz, J_{PH} = 4.3 Hz, 1H, H6), 2.06 (s, 3H, Me of guaiazulene), 1.99 (sept, J_{HH} = 6.6 Hz, 1H, CH of ^{i}Pr), 1.62 (s, 3H, Me of guaiazulene), 0.96 (d, J_{HH} = 6.6 Hz, 3H, Me of ^{i}Pr), 0.95 (d, J_{HH} = 9.0 Hz, 9H, PMe_3), 0.88 (d, J_{HH} = 6.6 Hz, 3H, Me of ^{i}Pr). ^{13}C{^{1}H} NMR: δ 217.4 (d, J_{PC} = 9.5 Hz, CO), 211.8 (CO), 206.2 (CO), 197.5 (d, J_{PC} = 9.5 Hz, CO), 148.5 (4°), 106.6 (C8), 102.2 (4°), 85.3 (4°), 84.7 (4°), 82.9 (C2), 81.4 (C5), 69.1 (4°), 73.2 (C3), 44.6 (C6), 38.5 (CH of ^{i}Pr), 22.8 (Me of ^{i}Pr), 23.6 (Me of guaiazulene), 21.6 (Me of ^{i}Pr), 19.3 (d, J_{PC} = 27 Hz, Me of PMe_3), 12.7 (Me of guaiazulene). ^{31}P{^{1}H} NMR: δ 4.14. IR (KBr, cm^{-1}): ν(CO) 1991, 1945, 1928, 1888. Anal. Calcd for $C_{22}H_{27}O_4PRu_2$: H, 4.59; C, 44.90. Found: H, 4.76; C, 44.45.

5g-A: yellow crystals, mp 143 °C (dec). ^{1}H NMR: δ 5.26 (d, J_{HH} = 2.4 Hz, 1H, H2), 5.22 (dd, J_{HH} = 8.2 Hz, J_{PH} = 5.0 Hz, 1H, H5), 5.15 (s, 1H, H8), 3.45 (d, J_{PH} = 4.5 Hz, 6H, CH_2 of P{$(OCH_2)_3$CMe}), 3.37 (d, J_{HH} = 2.4 Hz, 1H, H3), 3.31 (ddd, J_{HH} = 1.6, 8.2 Hz, J_{PH} = 5.0 Hz, 1H, H6), 2.07−2.03 (m, 1H, CH of ^{i}Pr), 2.02 (s, 3H, Me of guaiazulene), 1.86 (s, 3H, Me of guaiazulene), 1.00 (d, J_{HH} = 6.5 Hz, 3H, Me of ^{i}Pr), 0.94 (d,

(24) Wadsworth, W. S., Jr.; Emmons, W. D. *J. Am. Chem. Soc.* **1962**, *84*, 610.

J_{HH} = 6.5 Hz, 3H, Me of ^{i}Pr), −0.37 (s, 3H, Me of P{$(OCH_2)_3$CMe}). $^{13}C\{^1H\}$ NMR: δ 214.3 (br, CO), 211.6 (CO), 205.5 (CO), 194.2 (br, CO), 148.6 (4°), 107.1 (C8), 102.6 (4°), 86.4 (4°), 86.0 (4°), 83.6 (C2), 80.6 (C5), 75.4 (d, J_{PC} = 7.5 Hz, CH_2 of P{$(OCH_2)_3$CMe}), 74.1 (C3), 45.2 (C6), 38.4 (CH of ^{i}Pr), 31.9 (4°), 31.7 (4°), 23.6 (Me of guaiazulene), 22.7 (Me of ^{i}Pr), 21.5 (Me of ^{i}Pr), 14.0 (s, Me of P$(OCH_2)_3$CMe), 12.6 (Me of guaiazulene). $^{31}P\{^1H\}$ NMR: δ 121.8. IR (KBr, cm^{-1}): ν(CO) 2008, 1953, 1919, 1905. Anal. Calcd for $C_{24}H_{27}O_7PRu_2$: H, 4.09; C, 43.64. Found: H, 4.12; C, 43.20.

5h-A: yellow crystals; mp 168−171 °C (dec). ^{1}H NMR: δ 7.32 (d, J_{HH} = 8.6 Hz, 6H, *ortho*), 7.02 (dd, J_{HH} = 7.5, 8.6 Hz, 6H, *meta*), 6.85 (t, J_{HH} = 7.5 Hz, 3H, *para*), 5.22 (dd, J_{HH} = 8.2 Hz, J_{PH} = 5.4 Hz, 1H, H5), 5.13 (d, J_{HH} = 2.7 Hz, 1H, H2), 5.08 (s, 1H, H8), 3.23 (d, J_{HH} = 2.7 Hz, 1H, H3), 2.06 (ddd, J_{HH} = 1.2, 8.2 Hz, J_{PH} = 5.4 Hz, 1H, H6), 1.93 (s, 3H, Me of guaiazulene), 1.85 (sept, J = 6.6 Hz, 1H, CH of ^{i}Pr), 1.42 (s, 3H, Me of guaiazulene), 0.83 (d, J = 6.8 Hz, 3H, Me of ^{i}Pr), 0.76 (d, J = 6.8 Hz, 3H, Me of ^{i}Pr). $^{13}C\{^1H\}$ NMR: δ 216.0 (br, CO), 210.5 (CO), 204.9 (CO), 196.1 (br, CO), 152.0 (*ipso*), 149.1 (4°), 130.7 (*meta*), 125.3 (*ortho*), 121.3 (*para*), 107.0 (C8), 86.4 (4°), 85.8 (4°), 83.3 (C2), 80.6 (C5), 73.8 (C3), 70.8 (4°), 46.7 (C6), 31.9 (4°), 38.4 (CH of ^{i}Pr), 30.0 (Me of guaiazulene), 22.4 (Me of ^{i}Pr), 21.4 (Me of ^{i}Pr), 12.4 (Me of guaiazulene). $^{31}P\{^1H\}$ NMR: δ 127.4. IR (KBr, cm^{-1}): ν(CO) 2007, 1959, 1948, 1905. Anal. Calcd for $C_{37}H_{33}O_7PRu_2$: H, 4.01; C, 53.96. Found: H, 4.11; C, 54.23.

Preparation of 6a and Isolation of 2-A by Treatment of a Mixture of 2-A and 2-B with Phosphorus Ligands. In a typical example, a mixture of **2-A** and **2-B** (100 mg, 0.18 mmol) was dissolved in C_6H_6 (12 mL). PMe_3 (57.7 μL, 0.55 mmol) was added at room temperature, and the mixture was stirred in the dark for 3 h. After removal of the solvent and uncoordinated PMe_3, the resulting yellow oil was extracted with pentane. Concentration of the extracts afforded **2-A** as yellow crystals in 28% yield. Recrystallization of the residue from CH_2Cl_2/pentane (1:1) at −30 °C gave **6a** as yellow crystals (36.6 mg, 33%). Similar treatment of a mixture of **2-A** and **2-B** with 2−3 equiv of P{$(OCH_2)_3$CMe} or $P(OPh)_3$ at room temperature for 5 h gave a mixture of **2-A** and either **6g-A** or **6h-A**. After concentration of the reaction mixture, column chromatography {Al_2O_3 (φ 1.75 × 12 cm) at −10 °C} by eluting with a 10:1 mixture of hexane and CH_2Cl_2 gave a yellow band containing **2-A** (36−39%). A second yellow band containing **6g-A** or **6h-A** was available by eluting with a 4:1 mixture of hexane and CH_2Cl_2. Recrystallization of chromatographically purified **6g-A** or **6h-A** from a mixture of CH_2Cl_2 and pentane gave analytically pure **6g-A** or **6h-A** in 38 or 31% yield.

2-A: yellow crystals; mp 121−123 °C. ^{1}H NMR: δ 5.06 (d, J = 2.4 Hz, 1H, H3), 4.99 (d, J = 2.0 Hz, 1H, H8), 4.70 (d, J = 8.8 Hz, 1H, H5), 3.13 (d, J = 2.4 Hz, 1H, H2), 2.98 (dd, J = 1.5, 8.8 Hz, 1H, H6), 1.85 (s, 3H, Me of guaiazulene), 1.79 (sept, J = 6.8 Hz, 1H, CH of ^{i}Pr), 1.45 (s, 3H, Me of guaiazulene), 0.79 (d, J = 6.8 Hz, 3H, Me of ^{i}Pr), 0.75 (d, J = 6.8 Hz, 3H, Me of ^{i}Pr). $^{13}C\{^1H\}$ NMR: δ 209.4 (s, CO), 203.6 (s, CO) 146.7 (C7), 106.9 (C8), 103.0 (C1), 86.2 (C9), 85.3 (C10), 82.9 (C3), 79.6 (C5), 73.5 (C2), 73.0 (C4), 44.4 (C6), 37.0 (CH of ^{i}Pr), 22.7 (Me of guaiazulene), 21.3 (Me of ^{i}Pr), 20.3 (Me of ^{i}Pr), 11.2 (Me of guaiazulene). IR (KBr, cm^{-1}): ν(CO) 2042, 1988, 1972, 1911. Anal. Calcd for $C_{20}H_{18}O_5Ru_2$: H, 3.33; C, 44.44. Found: H, 3.41; C, 44.70.

6a-A: yellow crystals; mp 146−148 °C (dec). ^{1}H NMR: δ 5.66 (d, J = 7.8 Hz, 1H, H5), 5.26 (dd, J = 2.7, 7.8 Hz, 1H, H6), 5.09 (d, J = 2.9 Hz, 1H, H2), 4.92 (d, J = 2.9 Hz, 1H, H3), 3.18 (d, J = 6.2 Hz, 1H, H8), 2.69 (sept, J = 6.6 Hz, 1H, CH of ^{i}Pr), 1.78 (s, 3H, Me of guaiazulene), 1.35 (s, 3H, Me of guaiazulene), 1.28 (d, J = 6.6 Hz, 3H, Me of ^{i}Pr), 1.26 (d, J = 6.6 Hz, 3H, Me of ^{i}Pr), 1.12 (d, J = 9.0 Hz, 9H, PMe_3). $^{13}C\{^1H\}$ NMR: δ 159.9 (4°), 130.4 (4°), 130.0 (C5), 112.2 (C6), 96.7 (4°), 92.2 (4°), 86.0 (C2), 85.8 (4°), 80.0 (C3), 35.8 (CH of ^{i}Pr), 25.2 (Me of ^{i}Pr), 22.7 (Me of guaiazulene), 21.4 (Me of ^{i}Pr), 20.2 (d, J = 27 Hz, Me of PMe_3), 15.3 (C8), 10.6 (Me of guaiazulene). No peak due to the carbonyl ligands was observed in the carbonyl region of the ^{13}C NMR spectrum because of rapid site exchange of the CO ligands.[17] Variable-temperature measurement (from 40 to −60 °C) in the presence or absence of Cr(acac)$_3$ or application of longer pulse repetition time did not improve the situation. $^{31}P\{^1H\}$ NMR: δ −17.6. IR (KBr, cm^{-1}): ν(CO) 2037, 1971, 1952, 1940, 1897. Anal. Calcd for $C_{23}H_{27}O_5PRu_2$: H, 4.38; C, 44.81. Found: H, 4.34; C, 44.78.

6g-A: yellow crystals; mp 160 °C (dec). ^{1}H NMR: δ 5.62 (d, J = 7.8 Hz, 1H, H5), 5.24 (dd, J = 4.9, 7.8 Hz, 1H, H6), 5.14 (d, J = 2.9 Hz, 1H, H2), 4.97 (d, J = 2.9 Hz, 1H, H3), 3.42 (d, J = 4.8 Hz, 6H, CH_2 of P$(OCH_2)_3$CMe), 3.23 (d, J = 10.4 Hz, 1H, H8), 2.65 (sept, J = 6.8 Hz, 1H, CH of ^{i}Pr), 1.80 (s, 3H, Me of guaiazulene), 1.36 (s, 3H, Me of guaiazulene), 1.24 (d, J = 6.8 Hz, 3H, Me of ^{i}Pr), 1.23 (d, J = 6.8 Hz, 3H, Me of ^{i}Pr), −0.47 (s, 3H, Me of P$(OCH_2)_3$CMe). $^{13}C\{^1H\}$ NMR: δ 159.5 (4°), 129.9 (C5), 112.3 (C6), 96.3 (4°), 91.6 (4°), 85.8 (C2), 85.5 (4°), 79.5 (C3), 75.2 (d, J = 7.0 Hz, CH_2 of P{$(OCH_2)_3$CMe}), 35.8 (CH of ^{i}Pr), 31.5 (4°), 25.1 (Me of ^{i}Pr), 22.6 (Me of guaiazulene), 21.6 (Me of ^{i}Pr), 14.3 (s, Me of P{$(OCH_2)_3$CMe}), 15.6 (C8), 10.6 (Me of guaiazulene). No peak was observed in the carbonyl region of the ^{13}C NMR spectrum. $^{31}P\{^1H\}$ NMR: δ 134.6. IR (KBr, cm^{-1}): ν(CO) 2063, 2055, 1984, 1964, 1916. Anal. Calcd for $C_{25}H_{27}O_8PRu_2$: H, 3.92; C, 43.60. Found: H, 4.00; C, 43.73.

6h-A: yellow crystals; mp 137−138 °C (dec). ^{1}H NMR: δ 7.24 (d, J = 8.0 Hz, 6H, *o*-PhH), 6.94 (dd, J = 7.5, 8.0 Hz, 6H, *m*-PhH), 6.80 (t, J = 7.5 Hz, 3H, *p*-PhH), 5.64 (d, J = 7.3 Hz, 1H, H5), 5.25 (dd, J = 5.6, 7.3 Hz, 1H, H6), 5.10 (d, J = 2.9 Hz, 1H, H2), 4.94 (d, J = 2.9 Hz, 1H, H3), 3.14 (d, J = 10.4 Hz, 1H, H8), 2.42 (sept, J = 6.8 Hz, 1H, CH of ^{i}Pr), 1.86 (s, 3H, Me of guaiazulene), 1.37 (s, 3H, Me of guaiazulene), 1.13 (d, J = 6.8 Hz, 3H, Me of ^{i}Pr), 1.11 (d, J = 6.8 Hz, 3H, Me of ^{i}Pr). $^{13}C\{^1H\}$ NMR: δ 152.3 (4°), 149.1 (4°), 130.2 (*m*-Ph), 130.0 (C5), 125.3 (*o*-Ph), 121.8 (*p*-Ph), 113.1 (C6), 96.6 (4°), 86.7 (4°), 86.2 (C2), 80.6 (C3), 73.8 (4°), 38.4 (CH of ^{i}Pr), 30.0 (4°), 30.0 (Me of guaiazulene), 25.2 (Me of ^{i}Pr), 21.4 (Me of ^{i}Pr), 16.1 (C8), 12.4 (Me of guaiazulene). No peak was observed in the carbonyl region of the ^{13}C NMR spectrum. $^{31}P\{^1H\}$ NMR: δ 138.6. IR (KBr, cm^{-1}): ν(CO) 2054, 1993, 1982, 1963, 1910. Anal. Calcd for $C_{38}H_{33}O_8PRu_2$: H, 3.88; C, 53.64. Found: H, 3.96; C, 54.01.

Isolation of 2-B. A mixture of **2-A** and **2-B** (**2-A**:**2-B** = 68:32) was dissolved in CH_2Cl_2/pentane (1:1) and cooled at −30 °C. A small amount of pale orange crystals of **2-B** was manually taken from this mixture.

2-B: ^{1}H NMR δ 4.95 (d, J = 2.4 Hz, 1H, H2), 4.90 (d, J = 2.4 Hz, 1H, H3), 4.64 (dd, J = 1.5, 8.8 Hz, 1H, H5), 4.37 (d, J = 2.0 Hz, 1H, H8), 3.04 (dd, J = 2.0, 8.8, Hz, 1H, H6), 2.39 (sept, J = 6.8 Hz, 1H, CH of ^{i}Prs), 1.17 (Me of guaiazulene), 1.12 (d, J = 6.8 Hz, 3H, Me of ^{i}Pr), 1.10 (d, J = 6.8 Hz, 3H, Me of ^{i}Pr), 0.99 (Me of guaiazulene); $^{13}C\{^1H\}$ NMR δ 209.0 (s, 1C, CO), 203.3 (s, 1C, CO), 200.7 (br, 3C, CO), 124.5 (C5), 122.0 (C7), 108.3 (C4), 92.3 (C1), 86.6 (C10), 82.1 (C3), 80.2 (C2), 79.4 (C9), 49.8 (C8), 49.7 (C6), 36.5 (CH of ^{i}Pr), 26.5 (Me of ^{i}Pr), 19.0 (Me of guaiazulene), 17.4 (Me of ^{i}Pr), 9.2 (Me of guaiazulene); IR (KBr, cm^{-1}) ν(CO) 2043, 1985, 1973, 1910. Anal. Calcd for $C_{20}H_{18}O_5Ru_2$: H, 3.33; C, 44.44. Found: H, 3.41; C, 44.59.

Photoisomerization of 2-A to 2-B. A solution of **2-A** (1 mg, 0.002 mmol) in toluene-d_8 (0.4 mL, 0.05 M) was sealed in a 5 mm φ tube in vacuo. The solution was irradiated using a xenon lamp with interference filters (400, 500, and 600 ± 10 nm). The reactions were monitored several times using ^{1}H NMR spectroscopy. The ratios of **2-A** and **2-B** were independent of the wavelength.

Kinetic Study for Thermal Isomerization of 2-A to 2-B. The reactions were conducted in sealed tubes, and the concentration of the product was monitored periodically by ^{1}H NMR, with the temperature in the probe set at 308, 313, 318,

and 323 K. Experiments starting from pure **2-A** to **2-B** were carried out at different temperatures (308, 313, 318, 323 K). The data were treated in terms of reversible first-order kinetics: plots of $(x_e/a)\ \ln[x_e/(x_e - x)]$ (x_e, the concentration of the product in equilibrium; a, the initial concentration of the reactant; x, the concentration of the product at time t) vs time resulted in straight lines ($r > 0.99$). The rate constants $(k_1)_{obs}$ were extracted as the slopes of these lines. Plots of the logarithmic function of the rate constants vs the reciprocal of temperature gave typical Arrhenius plots, from which the activation parameters at 373 K were determined. Details are given in the Supporting Information.

Photochemical and Thermal Isomerization of 5g. A benzene-d_6 solution of **5g-A** (7 mg, 0.01 mmol) was irradiated in a sealed 5 mm ϕ tube in vacuo with a 450 W high-pressure Hg lamp. The reaction was monitored periodically using ^{1}H NMR spectroscopy. After 15 h, the yield of **5g-B** reached 28% based on the signal intensity of residual protons of C_6H_6. Some amounts (~4%) of byproducts including guaiazulene were also obtained. When the resulting solution containing **5g-A** and **5g-B** in a ratio of 72:28 was heated at 40, 60, 80, and 110 °C, **5g-B** was completely converted to **5g-A** after 18, 12, 8, and 3 h, respectively.

X-ray Data Collection and Reduction. Single crystals of **2-A**, **2-B**, **5g-A**, and **6a** were grown from a mixture of CH_2Cl_2 and pentane. X-ray crystallography measurement was performed on a Rigaku AFC-7R four-cycle axis diffractometer in the case of **2-B** and **5g-A** and was done on a Rigaku RAXIS II imaging plate diffractometer in the cases of **2-A** and **6a** with graphite-monochromated Mo Kα radiation ($\lambda = 0.71070$ Å). All data were collected at 223(2) K (**2-A** and **6a**) and 293(2) K (**2-B** and **5g-A**) using $\omega-2\theta$ technique to a maximum 2θ value of 60.1° (**2-A** and **6a**) and 55.0° (**2-B** and **5g-A**). The structures were solved by Patterson methods (DIRDIF94 PATTY) and were refined using full-matrix least-squares (SHELXL97-2) based on F^2 of all independent reflections measured. All H atoms were located at ideal positions and were included in the refinement, but were restricted to riding on the atom to which they were bonded. Isotopic thermal factors of H atoms were held to 1.2−1.5 times (for methyl groups) U_{eq} of the riding atoms.

Acknowledgment. A part of this study was financially supported by the Japan Society for the Promotion of Science (Grants-In-Aid for Scientific Research 10450343 and 12750768).

Supporting Information Available: Typical experimental detail and tables of spectroscopic data of **3a**−**h** and **4a**−**h**, figures of the NMR charts that support characterization of **5g-B**, tables of X-ray structural data, including data collection parameters, positional and thermal parameters, and bond lengths and angles for complexes **4e-A**, **5g-A**, **6a**, **2-A**, and **2-B**, and text giving experimental details for kinetics. This material is available free of charge via the Internet at http://pubs.acs.org.

OM000608G